

# Pulse glucometry: a new approach for noninvasive blood glucose measurement using instantaneous differential near-infrared spectrophotometry

**K. Yamakoshi**

Kanazawa University  
Graduate School of Natural Science  
and Technology  
Kanazawa 920-1192, Japan

**Y. Yamakoshi**

TYT Institute of Technology Corp.  
Kanazawa, Japan

**Abstract.** We describe a new optical method for noninvasive blood glucose (BGL) measurement. Optical methods are confounded by basal optical properties of tissues, especially water and other biochemical species, and by the very small glucose signal. We address these problems by using fast spectrophotometric analysis in a finger, deriving 100 transmittance spectra per second, to resolve optical spectra (900 to 1700 nm) of blood volume pulsations throughout the cardiac cycle. Difference spectra are calculated from the pulsatile signals, thereby eliminating the effects of bone, other tissues, and non-pulsatile blood. A partial least squares (PLS) model is used with the measured spectral data to predict BGL levels. Using glucose tolerance tests in 27 healthy volunteers, periodic optical measurements were made simultaneously with collection of blood samples for *in vitro* glucose analysis. Altogether, 603 paired data sets were obtained in all subjects and two-thirds of the data or of the subjects randomly selected were used for the PLS calibration model and the rest for the prediction. Bland-Altman and error-grid analyses of the predicted and measured BGL levels indicated clinically acceptable accuracy. We conclude that the new method, named pulse glucometry, has adequate performance for safe, noninvasive estimation of BGL. © 2006 Society of Photo-Optical Instrumentation Engineers. [DOI: 10.1117/1.2360919]

Keywords: spectrophotometry; biomedical optics; infrared spectroscopy.

Paper 05344R received Nov. 17, 2005; revised manuscript received Apr. 17, 2006; accepted for publication Jun. 22, 2006; published online Oct. 24, 2006.

## 1 Introduction

*In vivo* spectrophotometric analysis attracts attention due to its potential for allowing safe, convenient, noninvasive biochemical measurement. While the prospects for general biochemical analysis are often proposed and discussed, much of the attention has actually been focused on blood glucose (BGL) measurement because reliable BGL assessment is a vital part of self-care by the increasing number of diabetic patients worldwide. Optical methods aside, for more than four decades, improved BGL monitoring based on other principles has also been sought, in particular to eliminate the need for the frequent, often painful, finger pricking and blood analysis, which, even today, remains the most widely used method. Over this period, several potential alternatives have emerged including invasive implantable microsensors,<sup>1,2</sup> the minimally invasive procedure of skin microporation using a laser or miniaturized lancets,<sup>3</sup> as well as transdermal measurement based on extraction of interstitial fluids through the skin using iontophoresis<sup>4,5</sup> or sonophoresis.<sup>6</sup> The subject has been reviewed by several authors; see, for example, Ref. 7.

A truly noninvasive BGL measurement technique has been sought for many years and optical methods in general have appeared to offer very strong prospects for achieving this.<sup>8-10</sup> These optical methods have included the measurement of the rotation of optical polarization in the aqueous humor of the eye<sup>11,12</sup> or a colorimetric contact lens measuring in tear film<sup>13</sup> or the use of near-infrared spectroscopy (NIRS) in tissues, such as the finger or the lip.<sup>14,15</sup> Raman spectroscopy has also been investigated for this purpose.<sup>16</sup> Most of these methods have been explored widely but to date, apparently none has provided sufficiently precise and accurate measurements for reliable clinical use.<sup>14</sup> The obstacles to success with *in vivo* NIRS for BGL measurement are, on the one hand, the very small *in vivo* spectral signal of glucose, and on the other hand, the combination of interference from other absorbing species; multiple scatter in skin, muscle, and bone; and the strong absorption bands of water.<sup>9,17,18</sup> Indeed, the optical absorption spectrum of water effectively masks glucose absorption bands as determined with conventional NIR spectrophotometers. There are clearly substantial difficulties in using spectroscopic techniques for noninvasive measurement of glucose not the least of which is that often methods used for assessing the validity of a given technique are not fully described by authors, as reported by Arnold and Small.<sup>18</sup>

Address all correspondence to Prof. Ken-ichi Yamakoshi, Graduate School of Natural Science and Technology, Kanazawa University, Kakuma, Kanazawa 920-1192, Japan; Tel: +81-(0)76-234-4735; Fax: +81-(0)76-234-4739; E-mail: yamakosi@t.kanazawa-u.ac.jp

We have recently designed a novel NIRS technique,<sup>19</sup> which we term *pulse glucometry*. This method has been designed to minimize or remove influences of many of the confounding factors by collecting optical data from pulsatile blood volume changes in tissue. There is a substantial amount of literature describing uses of photoplethysmography for monitoring several physiological variables, such as blood volume and flow, oxygen saturation, and blood constituents, such as glucose.<sup>15,20-23</sup> The invention of pulse oximetry by Aoyagi<sup>24,25</sup> has had the most important clinical impact of all of these developments to date. The essence of this technique is to make photoplethysmographic measurements of arterial blood volume pulsations, typically at two wavelengths, one in the red and the other in the infrared parts of the spectrum, then to derive simple ratios of these measurements to determine the relative proportions of the two most significant chromophores oxy- and deoxyhemoglobin. The patent literature reveals many attempts to use spectrophotometric techniques to measure BGL and a method based on two-wavelength analysis of the arterial pulse signal has been proposed.<sup>26</sup> These authors claim that the invention uses one wavelength, which is “glucose sensitive,” and a second wavelength, which is “glucose insensitive,” then, as with pulse oximetry, to use ratios of pulsatile-to-continuous components of the photoplethysmogram at each wavelength to derive an estimate of glucose concentration. Although this invention was classified as a granted patent in 1992, no instrument has yet been made available for use. In fact, this situation is characteristic of the noninvasive glucose monitoring field, where numerous granted patents exist and no clinically accepted instrument is yet available.

This paper represents our first description of pulse glucometry together with preliminary *in vivo* results. There is clearly much more research to be done before all technical and clinical aspects of our method have been fully investigated. For example, we must thoroughly investigate further the performance of the chemometric methods of analysis that we have used, since there are many possible shortcomings as pointed out by others.<sup>15,18</sup> Nevertheless, we feel that the results obtained to date are sufficiently encouraging to report the method as one worthy of serious consideration in this field of noninvasive BGL monitoring.

## 2 Basic Principle of the Measurement

The method described here utilizes spectrophotometric analysis in a tissue segment, such as a finger. Glucose exhibits several absorption bands between 0.7 and 2.5  $\mu\text{m}$  and within this range it is important that there are broad and strong water absorption bands at 1.45 and 1.92  $\mu\text{m}$ .<sup>27</sup> In order to avoid these bands, it is theoretically possible to use the combination region (2.0 to 2.5  $\mu\text{m}$ ), the first overtone region (1.54 to 1.82  $\mu\text{m}$ ) and the near-infrared region (0.7 to 1.33  $\mu\text{m}$ ). Glucose exhibits three absorption bands in each of these regions: 2.10, 2.27, and 2.32  $\mu\text{m}$  in the combination region; 1.73, 1.69, and 1.61  $\mu\text{m}$  in the first overtone region; and 0.76, 0.92, and 1.00  $\mu\text{m}$  in the near-infrared region. Of these glucose absorption bands, the latter in the near-infrared region are particularly weak.<sup>14,15</sup> To recover the glucose information in tissue having high water content, multivariate analysis covering a suitable region of the optical spectrum must be used.

The essence of our new approach is to utilize a blood volume change in a tissue segment under optical interrogation, such as a finger, and then, with a subtraction process, to derive changes in optical density (OD) to remove the influences of basal interfering elements.

We assume a simplified model of the tissue under interrogation, as shown in Fig. 1(a). This optical model comprises three compartments: arterial, venous, and bloodless tissue. The optical interrogation of the tissue is carried out with a broad-spectrum light source having incident radiation intensity  $I_0$  with the wavelength  $\lambda$ . Following absorption and scattering in each compartment, we have transmitted radiation intensity,  $I_\lambda$ . The arterial blood volume changes in a pulsatile way throughout the cardiac cycle, thereby producing small changes in the transmitted intensity,  $\Delta I_\lambda$ . If the transmitted intensity,  $I_\lambda$ , is detected periodically at time intervals  $\Delta t$  during the cardiac cycle, we obtain a time series for  $I_\lambda$

$$I_\lambda(t) = [I_\lambda(t_1), I_\lambda(t_2), \dots, I_\lambda(t_n)] \quad (1)$$

and,

$$\Delta t = t_{i+1} - t_i. \quad (2)$$

The time series will effectively represent the cardiac-related pulsatile intensity change superimposed upon the basal component, which relates to venous blood, bloodless tissue, and nonpulsatile arterial blood. Differences between the optical densities at successive time intervals can then be obtained, since

$$\text{OD}_\lambda = \log[I_0/I_\lambda(t_i)], \quad (3)$$

$$\text{OD}'_\lambda = \log[I_0/I_\lambda(t_{i+1})]. \quad (4)$$

Subtracting  $\text{OD}_\lambda$  from  $\text{OD}'_\lambda$ , we can obtain the difference of optical density at time  $t_i$ ,  $\Delta\text{OD}_\lambda$ , as

$$\Delta\text{OD}_\lambda = \log \frac{I_\lambda(t_i)}{I_\lambda(t_{i+1})} = \log \left( 1 + \frac{\Delta I_\lambda(t_i)}{I_\lambda(t_{i+1})} \right), \quad (5)$$

where,  $I_\lambda(t_i) = I_\lambda(t_{i+1}) + \Delta I_\lambda(t_i)$ .

This subtraction has the effect of removing the venous and the tissue contributions to yield only the change in intensity due to the pulsating arterial blood compartment. Now, if the transmitted radiation is spectrally resolved into its component individual wavelengths, it will be possible to recover a family of time series, each member displaying the pulsatile intensity change present at one wavelength, as shown in Fig. 1(b). In order to implement this general principle in practice, we use the peak-to-peak magnitude of each cardiac-related pulse. The magnitudes of the cardiac-related pulsatile intensity components at wavelengths  $\lambda_1, \lambda_2, \dots, \lambda_n$  are given as  $\Delta I_{\lambda_1}, \Delta I_{\lambda_2}, \dots, \Delta I_{\lambda_n}$ . Based on Eq. (5), we can then convert these into changes in optical density  $\Delta\text{OD}_{\lambda_1}, \Delta\text{OD}_{\lambda_2}, \dots, \Delta\text{OD}_{\lambda_n}$ .

These data can also be viewed as spectra, for example, over a near-infrared range with  $\Delta\text{OD}_\lambda$  plotted against wavelength  $\lambda$ . If such spectra are derived at different levels of BGL concentration,  $\text{BGL}_i$ , we will obtain a family of spectra, as is illustrated schematically in Fig. 1 (lower part), which may

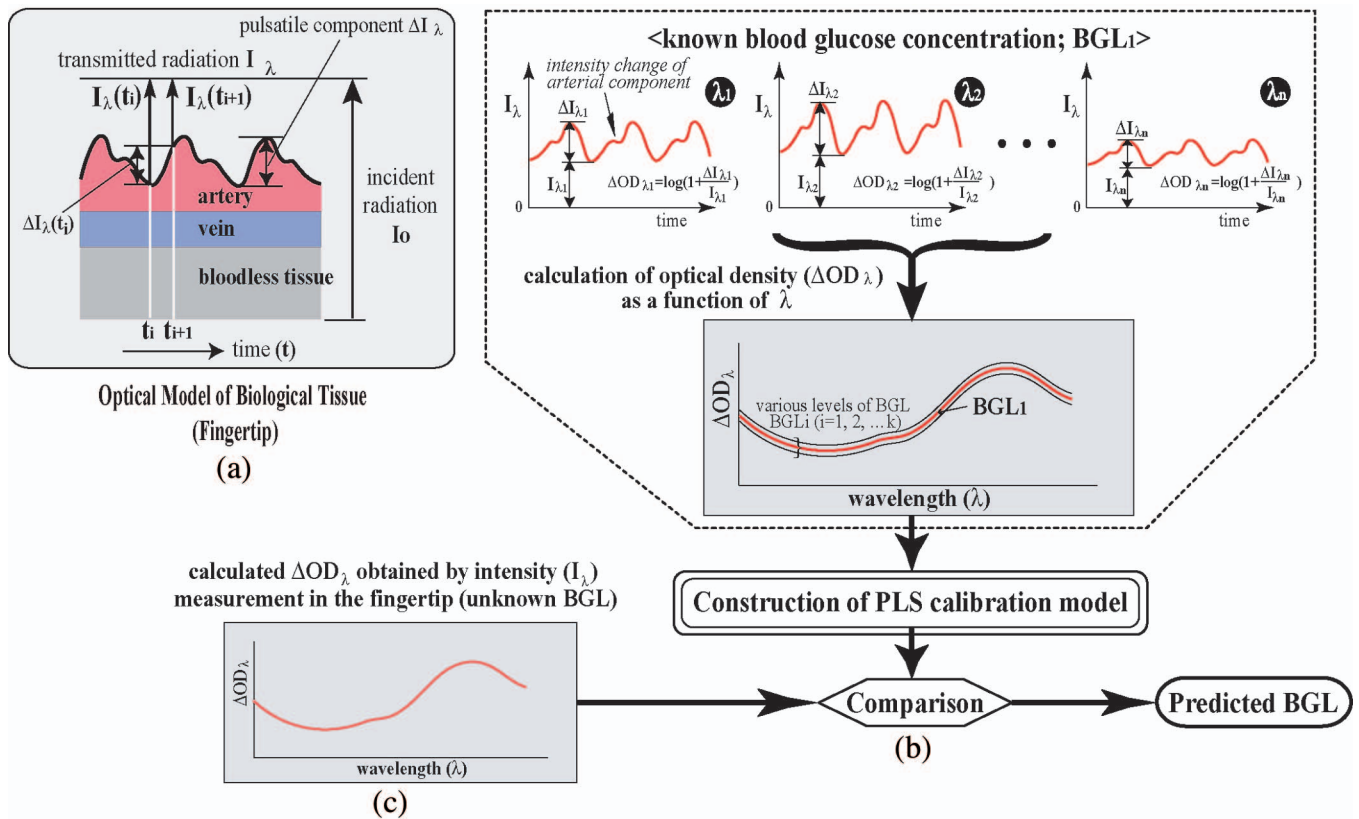


**Fig. 1** Basic principle of noninvasive measurement of blood glucose concentration (BGL) using instantaneous differential near-infrared spectrophotometry. Optical model of the biological tissue (fingertip) is shown (a). See text for explanation.

then be used for a multivariate analysis. As is common in multicomponent spectrophotometric analysis, we use a partial least squares (PLS) calibration model to obtain predictions of BGL.<sup>8-10,15,18,23,27,28</sup> The PLS model is first constructed by measuring BGL directly together with noninvasive optical measurements in a representative population. Then, for a given subject, spectra of  $\Delta OD_\lambda$  versus  $\lambda$  for the unknown

BGL values derived from *in vivo* measurements are compared with the PLS-derived calibration model and predicted BGL values are thereby calculated.

### 3 Materials and Methods

In order to obtain an instantaneous spectrum of the transmitted radiation through the tissue, we have developed a new,

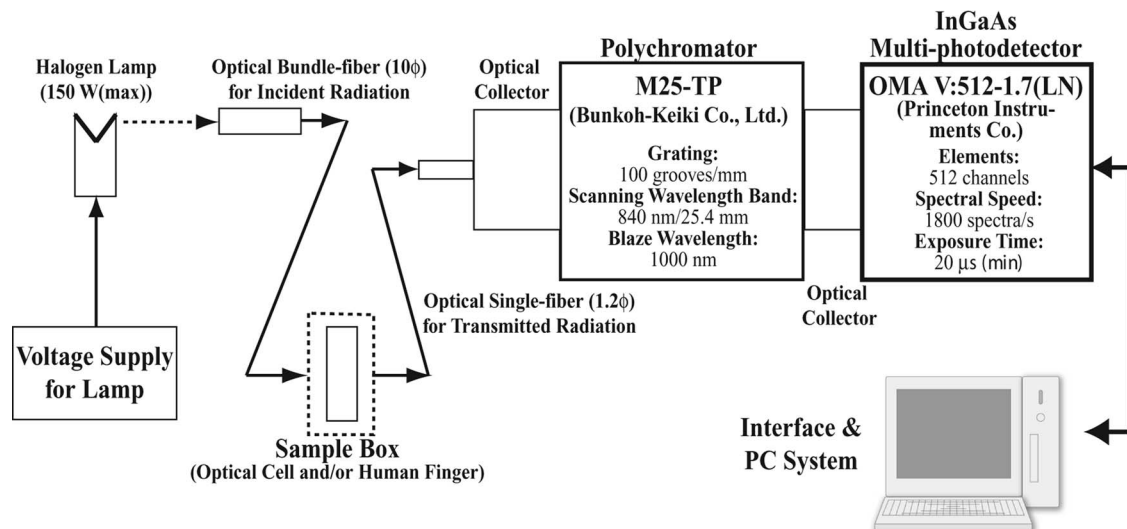


**Fig. 2** Block diagram of the high-speed near-infrared spectrophotometric system. See text for details.

fast, spectrophotometer. Figure 2 shows a block diagram of this system. It comprises a light source (halogen lamp: maximum power 150 W), an optical fiber bundle of 10-mm diameter for the incident radiation and a single fiber of 1.2-mm diameter for receiving the transmitted radiation, a spectrometer (polychromator, M25-TP; Bunkoh-Keiki Co. Ltd., Japan), a linear, liquid nitrogen cooled ( $-50$  to  $-100$  °C), InGaAs photodiode-array (multi-photodetector, OMA V: 512-1.7(LN); Princeton Instruments Co., USA), and a conventional personal computer with an appropriate interface. The spectrometer covers an effective wavelength range from 900 to 1700 nm with a resolution of better than 8 nm, and it has a maximum spectral rate of 1800 spectra/s with 1-MHz digitization (16 bits), and a minimum exposure time of 20  $\mu$ s. A key component of our instrument is the multi-photodetector. The model we used has a particularly high specification, and in terms of dark current, linearity, and stability, it is at present probably one of the best commercially available worldwide (see detailed information at [http://architect.wwwcomm.com/Uploads/Princeton/Documents/Datasheets/omav\\_512-17ln.pdf](http://architect.wwwcomm.com/Uploads/Princeton/Documents/Datasheets/omav_512-17ln.pdf)).

The spectral noise of the instrument was evaluated both *in vitro* and *in vivo*. First, for the *in vitro* assessment, we recorded sequential transmission spectra from a 1.0-mm cuvette containing water and then calculated the difference between sequential pairs of spectra. This indicated a spectral noise value of 20  $\mu$ AU over the chosen operating wavelength range from 900 to 1700 nm. We then inserted a neutral density filter having an attenuation of 2.0 AU into the optical path, in addition to the 1.0-mm cuvette containing water, and once again repeated the acquisition of sequential spectra together with calculation of the difference spectra. This gave us a spectral noise value of around 30  $\mu$ AU over the same wavelength range. Second, we acquired sequential transmission spectra from a fingertip while an occlusion cuff was applied around the basal phalanx of the finger to halt blood circulation for a period of about 5 s. Once again, this allowed us to derive difference spectra from the sequential pairs of transmission spectra to determine the spectral noise value, but it also enabled us to assess stability and repeatability over the 5-s period. The spectral noise level was found to be around 30  $\mu$ AU over the wavelength range of 900 to 1700 nm. For about 50 sequential measurements made over the 5-s period, with an exposure time of 10 ms in the multi-photodetector, we found a spectral noise variation of around 0.5%.

In order to carry out *in vivo* measurements, glucose tolerance tests were carried out in 27 healthy volunteers (20 to 43 years old; 24 males and 3 females) after obtaining informed consent. The subjects were asked to abstain from food and alcohol from 9 p.m. on the previous day until the end of the experiment on the next morning. The experiment began at 9 a.m. in a temperature-controlled room held at 25 °C. During the experiment, the subjects were requested to sit quietly in a chair to undergo the test. Radiation intensity measurements were made in the left index fingertip at regular intervals before and after oral administration of glucose solution (75 g/225 ml, Trelan-G75, Shimizu Seiyaku, Co. Ltd., Japan) for a study period of 120 min. During the optical measurement, the subject's left hand was held horizontally at heart level. In some subjects, the interval between optical measure-

ments was 10 min, and in the remainder, the interval was 5 min. Immediately after each optical measurement blood samples (about 3 ml) were collected from the cephalic vein of the left forearm. The sampled blood was immediately analyzed by an automatic blood analyzer (DRI-CHEM 7000, Fujifilm Medical Co. Ltd., Japan) to obtain the reference BGL value (measured BGL). The analyzer uses a colorimetric principle based on glucose oxidase contained within single-use multilayer film elements. Quality control data accompanying each film element are entered into the analyzer, thereby ensuring automatic updating of calibration with every use.

For the optical intensity measurements, the fingertip was placed carefully in an adjustable space between the ends of the transmitting and receiving fibers so as to contact softly with the skin (see the inset in Fig. 3). The intensity measurements were made for about 20 to 30 s (about 20 to 30 cardiac pulses), spectra being gathered at a rate of 100  $s^{-1}$ . These conditions could achieve a measurement of the pulse component signal ( $\Delta I_\lambda$ ) superimposed on the intensity ( $I_\lambda$ ) with a signal-to-noise ratio (SNR) of more than 25 dB over the wavelength range from 900 to 1400 nm and approximately 22 dB from 1400 to 1700 nm. In the calculation of the change in absorbance ( $\Delta OD_\lambda$ ), however, since we have confirmed this SNR to be more than 20 dB above 1400 nm, we believe that the calculated  $\Delta OD_\lambda$  is sufficiently accurate within the range from 900 to 1700 nm. In order to gain an impression of the instrument noise level, we can see from the spectra shown in Fig. 4 that there is noise just discernible on the tracing, especially at higher wavelengths.

In each subject during the 120-min study period, 13 (10-min intervals) or 25 (5-min intervals) sets of the intensity measurements were made while the BGL was changing; the measured BGL values varied from about 80 to 220 mg/dl in all of the subjects. The beat-by-beat spectral data of blood ( $\Delta OD_\lambda$ ) against a measured BGL were calculated to obtain an averaged spectral curve of  $\Delta OD_\lambda$  obtained from stable and almost similar waveforms of the pulsatile intensity changes of 3 to 5 consecutive cardiac beats during the measurement interval of 20 to 30 s. The spectrum of  $\Delta OD_\lambda$  was then normalized, using the value of the  $\Delta OD_\lambda$  at 900 nm as 1.0, together with the minimum value of  $\Delta OD_\lambda$  as 0. Thus 603 paired data sets of the measured BGL values and the normalized spectra of  $\Delta OD_\lambda$  were obtained from the 27 healthy volunteers for use in the PLS modeling for which we employed the MATLAB™ PLS Toolbox 3.5 (Eigenvector Inc., USA). We have used two-thirds of the data for deriving the PLS calibration model and the remaining one-third for prediction. Two methods for selecting the data were used: In method A, we randomly selected 402 data sets for calibration and used the remaining 201 data sets for prediction. In method B, we randomly selected 18 subjects, using all of their data for calibration, leaving the data from the remaining 9 subjects for prediction. The analysis based on method B then allowed us to plot the time course of predicted and measured BGL in any of the nine subjects.

## 4 Results

The optical data collected during each 20 to 30 s measurement period allowed transmittance spectra to be plotted and for the temporal changes throughout each cardiac cycle to be

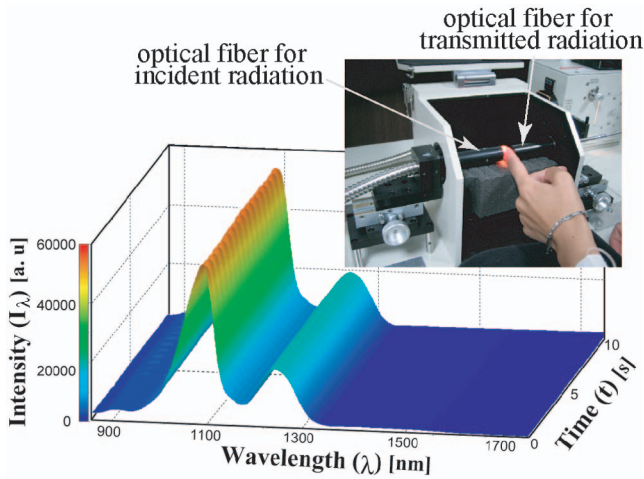


**Fig. 3** An example of a three-dimensional display of transmitted radiation intensity ( $I_\lambda$ ), wavelength ( $\lambda$ ), and time ( $t$ ) measured in the fingertip. Measuring scene is shown in the inset.

seen. Figure 3 shows an example of a three-dimensional representation of the transmitted radiation intensity in arbitrary units (a.u.) [ $I_\lambda$  a.u.] vertical axis  $y$ ] versus wavelength  $\lambda$  [nm] horizontal axis  $x$ ] and versus time  $t$  [(s) horizontal axis  $z$ ] measured in the fingertip of a female subject. From these transmittance spectra, it can be seen that the intensity exhibits a peak around 1100 nm and it is considerably decreased beyond approximately 1200 nm due to the strong absorption by the water component in the tissue, including blood. Pulsatile intensity changes with time, being of cardiac origin, can be seen as a “ripple” on the peak intensity at 1100 nm. These pulsatile changes are then shown more clearly in Fig. 4 for specific wavelengths at 100 nm intervals from 900 to 1700 nm. The PLS models were assessed by examination of the regression coefficient vectors.<sup>9,10,15,18,28</sup> The presence of positive peaks in the regression coefficients was seen in the spectral regions associated with glucose absorption indicating that these wavelengths have positive correlations to the tissue glucose content.

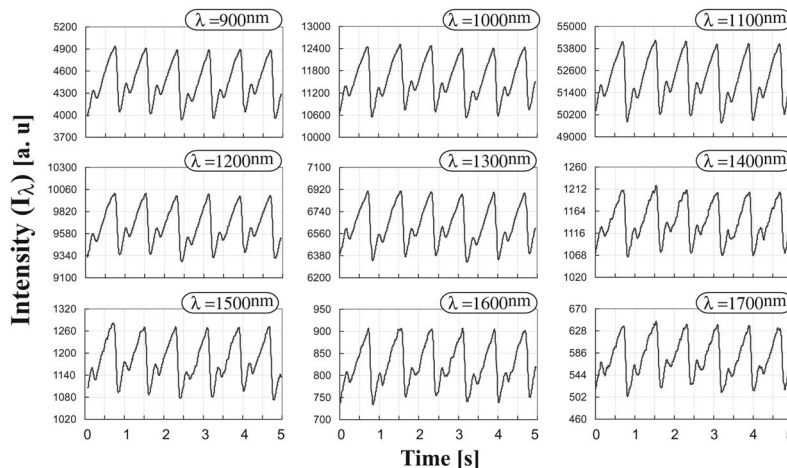


**Fig. 4** Examples of pulsatile component ( $\Delta I_\lambda$ ) records superimposed on the transmitted radiation intensity ( $I_\lambda$ ) measured from  $\lambda = 900$  to 1700 nm every 100-nm step obtained in the fingertip of the same subject in Fig. 3.

As mentioned above, we used two methods for selecting sets of data for model calibration and prediction, method A involving the random selection of 402 data sets from the total 603 data sets and method B in which we randomly selected 18 subjects, using all of their data for calibration and the data from the remaining 9 subjects for prediction. Method B allows the time course of measured and predicted BGL levels to be plotted for each individual subject and a typical example of such a time course of measured BGL levels (Fuji DRI-CHEM) before and after administration of glucose solution is shown in Fig. 5(a). Using the pulsatile intensity measurements as shown in Fig. 4, the corresponding optical density changes,  $\Delta OD_\lambda$ , were calculated for the whole spectral range and were then averaged for the measured cardiac beats to obtain a spectral curve of  $\Delta OD_\lambda$ : Standard deviations (SDs) of the averaged  $\Delta OD_\lambda$  spectral curves were within 1% between 900 and 1300 nm and were within about 2% beyond 1300 nm for the various BGL levels in the present glucose tolerance tests. An example of the averaged  $\Delta OD_\lambda$  obtained from four consecutive cardiac beats is shown in Fig. 5(b), which corresponds to time point I in Fig. 5(a). This procedure was repeated for all of the data collected during the glucose tolerance test, and the resulting spectra corresponding to the BGL values at time points I, II, III, and IV are normalized and are shown in Fig. 5(c). Predicted values of BGL were subsequently calculated using the PLS model and are also plotted in Fig. 5(a) together with the blood analysis results.

For both method A and method B, the paired data sets of the measured (Fuji DRI-CHEM) and predicted (pulse glucometry) BGL values were analyzed by the Bland-Altman method<sup>29</sup> and also using error-grid analysis.<sup>30</sup> The result of the Bland-Altman analysis for 201 paired data from method A, corresponding to a range in measured BGL values from 93 to 216 mg/dl, is shown in Fig. 6. The bias and precision of the predictions obtained by pulse glucometry as compared with direct blood analysis averaged  $1.22 \pm 22.3$  (mean  $\pm$  SD) mg/dl. Using method B, with 129 paired data corresponding to a range in measured BGL values from 93 to 211 mg/dl, we found a bias and precision of  $-2.48 \pm 21.9$  (mean  $\pm$  SD) mg/dl.

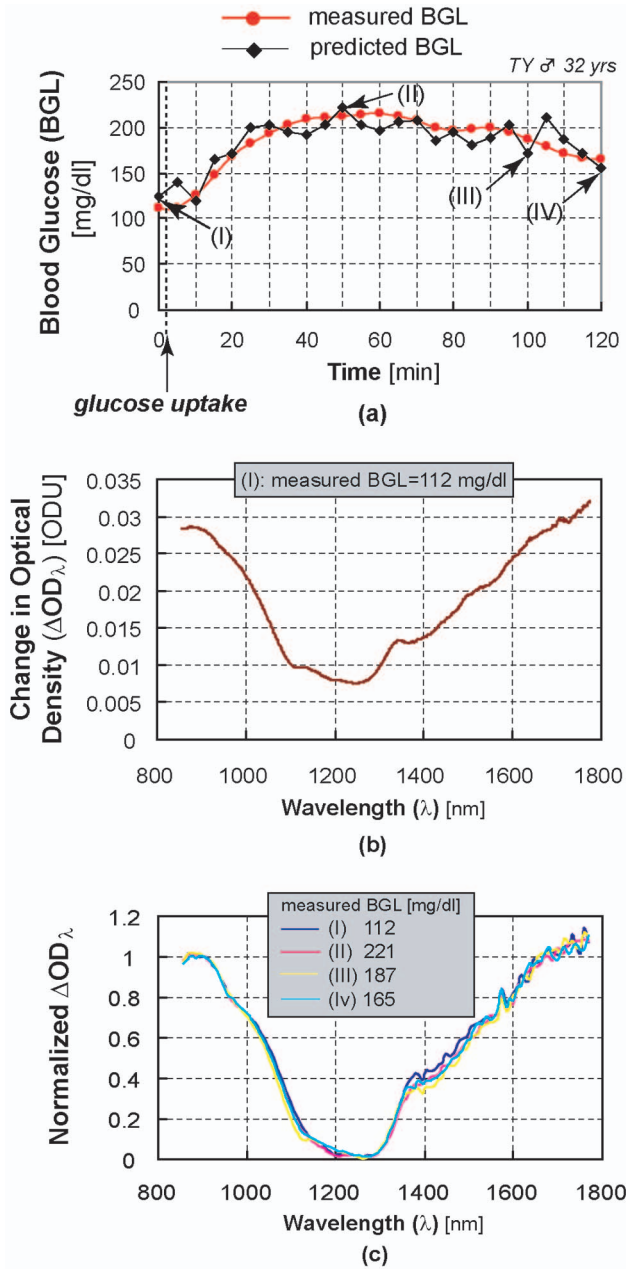


**Fig. 5** (a) An example of the time course of the measured and predicted BGL values before and after oral administration of glucose solution indicated by the arrow, (b) averaged spectrum of optical density ( $\Delta OD_{\lambda}$ ) obtained from four consecutive cardiac beats at a point I in (a) calculated from the light intensities ( $I_{\lambda}$  and  $\Delta I_{\lambda}$ ), and (c)  $\Delta OD_{\lambda}$  spectra which was normalized using the value of the  $\Delta OD_{\lambda}$  at 900 nm as 1.0 together with the minimum value of  $\Delta OD_{\lambda}$  as 0 in each calculated spectrum obtained at the points I, II, III, and IV in (a). The time course was obtained from the analysis based on method B.

The error-grid for the results of method A is shown in Fig. 7. This indicates that 181 data pairs (90.05%) fell within region A, and 20 data pairs (9.95%) fell within region B. The error-grid analysis for method B showed that 119 data pairs (92.2%) fell within range A and 10 data pairs (7.8%) fell within range B.

These results indicate that, for both methods of analysis (A and B), the new method, pulse glucometry, was able to pro-

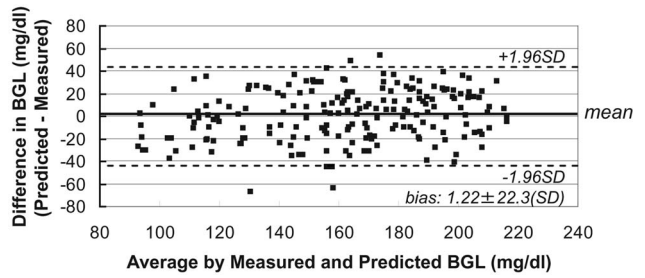


**Fig. 6** Difference between predicted and measured BGL values plotted against their average (Bland-Altman plot) analyzed by method A. See text for further explanation.

duce BGL estimates with precision and accuracy suitable for clinical purposes.

### 5 Discussion

The development of a reliable and convenient noninvasive method for BGL monitoring in order to avoid the need for blood sampling has been the focus of intense efforts for several decades.<sup>1,3</sup> Among the possible noninvasive approaches, those based on optical methods have seemed attractive but to date there has been no report of an entirely successful instrument.<sup>31</sup> *In vivo* spectrophotometric analysis is confounded by a number of factors, especially the influences of absorption and scatter by numerous tissue components, such as water, bone, muscle, skin, and the very many chemical constituents in blood other than glucose.<sup>17</sup> The strong absorption bands of water make the specific extraction of glucose absorption data technically difficult. Our approach is to utilize a change in the blood volume of an interrogated tissue segment, such as a fingertip, produced by the cardiac-related pulse to eliminate the basal interfering components. This approach may be compared with the widely used method of pulse oximetry, which uses two specific wavelengths for oxygen saturation monitoring.<sup>32</sup> In this connection, Heise et al.<sup>15</sup> suggested the possible use of diffuse reflectance spectroscopy for glucose measurement on human oral mucosa and that pulsatile absor-

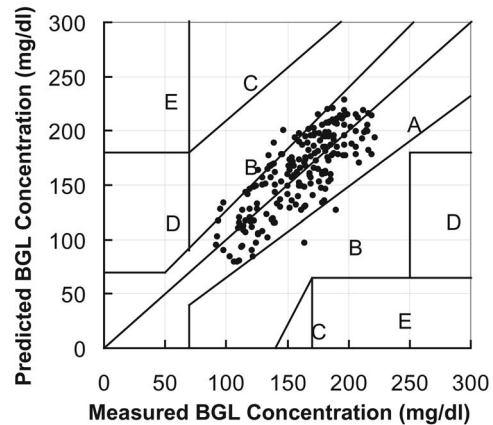


**Fig. 7** A scatter diagram showing comparison of the predicted and measured BGL values by error-grid analysis obtained by method A. Values in regions A and B are acceptable for clinical use. See text for explanation.

bance spectral measurement might be further investigated. These authors were unable to measure pulsatile spectra on the lip, there apparently being problems of the spectral SNR as well as inadequate time resolution of their instrumentation.

We have used venous blood samples for the construction of our PLS model, since venous blood sampling is used clinically and arterial blood sampling was felt not to be justified in healthy volunteers. We have noted optical intensity changes reflecting venous blood volume changes with breathing. It is theoretically possible to use these intensity changes to calculate BGL levels, but the signals are not as clear and reliable as the arterial blood volume pulsations. It is known that arterial BGL values may be 10 to 20% higher, or more, than venous BGL values.<sup>33</sup>

We have designed and constructed a spectrophotometric measurement system that is capable of deriving transmittance spectra from an adult human finger at sufficiently high speed to reveal cardiac-related pulsatile spectra over the near-infrared spectrum from 900 to 1700 nm. Reported *in vitro* absorption spectra of whole blood exhibit a large peak at around 1450 nm due to water. Interestingly, we found that the *in vivo* spectrum of the pulsatile blood compartment, as shown in Figs. 5(b) and 5(c), is consistently and markedly different to the *in vitro* spectrum, especially in the wavelength range beyond 1300 nm. The reasons for this are at present unclear. However, in their paper on time-resolved near-infrared spectroscopy, Nahm and Gehring<sup>22</sup> reported so-called "static" and pulsatile parts of finger tip optical density over the wavelength range from 600 to 1012 nm (16 667 to 9880  $\text{cm}^{-1}$ ). The static spectrum reveals the known water absorption band around 966 nm, with a magnitude of approximately 0.6 OD units (ODU or AU). However, the water absorption band is missing in the spectrum derived from pulsatile signals, which only reveals a part of the hemoglobin spectrum appearing between 643 and 602 nm. These authors do not give a detailed explanation for this finding, merely stating that it can be explained by a strong influence of extravascular water on the static spectrum, but no estimates for the relative proportions of the intravascular and extravascular compartments in the fingertip are given. These authors use a multilayer model of tissue comprising bloodless tissue, intravenous space, and intra-arterial space. This model assumes, first, that scattering effects are ignored and, second, that changes in optical density due to cardiac-related pulsatile blood volume are created by changes in the path length of the intra-arterial space. Although it is not clear from the description of their experimental arrangement, we assume that the positioning of their optical fibers for the incident and transmitted radiation is such that the finger is free to change diameter during the pulsatile changes in volume/path length. By contrast with their arrangement, we specifically ensure that our optical fibers are fixed in gentle contact with the opposing surfaces of the finger such that the intrafiber distance, and therefore the finger diameter, cannot change during the arterial pulse. In this case, any changes in intra-arterial volume must be compensated for by opposite changes in intravenous space. A simple analysis of this situation, bearing in mind that we derive difference spectra, suggests that this may lead to subtraction of the water spectrum. The obvious limitation of this simple analysis is that it does not fully account for

changes in attenuation across the finger caused by scattering phenomena, and we will study this further in our on-going research, but we now discuss scattering aspects further.

With respect to the matter of water absorption bands and to the critical issues of selectivity and choice of spectral range, it is inevitable that scattering phenomena play an important role. Amerov et al.<sup>28</sup> show in their *in vitro* studies of blood that the influence of glucose concentration on scattering is the dominant factor in what they refer to as the short-wavelength region. Their work elegantly shows that, *in vitro*, the most important mechanism is that of the influence of glucose uptake by blood cells on refractive index. In defining the three spectral ranges for their studies, they do not make a clear distinction between the first-overtone range and the short-wavelength range, simply stating that both are included in the range spanning from 9000 to 5400  $\text{cm}^{-1}$  (1.11 to 1.851  $\mu\text{m}$ ). They do, nevertheless, demonstrate much greater statistical variation in the glucose concentration correlation plot when using a PLS calibration model with spectral information restricted to the narrow spectral region from 8500 to 7300  $\text{cm}^{-1}$  (1.176 to 1.369  $\mu\text{m}$ ). The measurements reported in our present paper, which were *in vivo* whole tissue not merely *in vitro* blood samples, were actually made over the range of 11 111 to 5882  $\text{cm}^{-1}$  (900 to 1700 nm). We therefore include both the first-overtone range and the restricted short-wavelength range used by Amerov et al. It is not clear at this stage what effect this has on the performance of our instrument for BGL predictions and the implications of this will be fully investigated in our future research. Suffice it to say that we believe that the influences of scatter are much more complex in the *in vivo* situation as compared with the *in vitro* model.

The choice of spectral range is important for two reasons: First, it obviously influences the ability to recognize the target molecule from its known absorption bands amid other absorbing species. Second, it requires consideration of the likely wavelength-dependent effects of scattering phenomena that have a profound influence on optical path length. The matter of optical path length is critical in any attempt to derive quantitative measurements using spectrophotometry and this is especially important for *in vivo* determinations. Multiple scatter by tissues is a well-known and extensively studied phenomenon and many groups have made measurements of effective optical path length.<sup>17</sup> Actual optical path length estimates in some tissues can be made, with varying degrees of precision and accuracy, by using what has been defined as the optical path length factor  $\zeta$ , which is given by the relationship  $L_o = \zeta L$ , where  $L_o$  is the optical path length and  $L$  is the physical path length.<sup>17</sup> Some authors refer to this as the differential path length factor. Measurements of  $\zeta$  have been made in various tissues and, for example, the human brain has  $\zeta$  ranging from 4 to 5.  $\zeta$  for the adult fingertip is of a similar magnitude so that if the physical path length of the fingertip is 10 mm, the optical path length could be as much as 50 mm. This clearly has a significant impact on quantitative estimates using spectrophotometric methods.

Several authors, using either time-resolved or frequency domain measurements to measure the reduced scattering coefficient of various tissues (vascular and avascular), have reported wavelength-dependence following classical Mie

theory.<sup>34,35</sup> Recent studies in the human fingertip over the range 850 to 1050 nm actually show clearly the expected linear fall in reduced scattering coefficient with increasing wavelength.<sup>36</sup> Propagation of radiation through tissues is thus, naturally, influenced by wavelength, but is also influenced by the positioning of interrogating fibers and by applied pressure.<sup>37</sup> In diffuse reflectance measurements, which are now popular for BGL determinations, the penetration depth and therefore the interrogated volume are related to the geometrical spacing between transmitting and receiving fibers.<sup>10</sup>

In common with many others using NIRS for either non-invasive chemical measurement or *in vitro* analysis, we have used the multivariate statistical method of PLS regression. Although this method has the potential to provide meaningful predictions, great care is needed since it has been suggested that chance correlations can produce highly misleading results.<sup>14,15,18,31</sup> It has also been shown that use of time-correlated data as in conventional glucose tolerance tests can lead to false claims of model functionality.<sup>38</sup> Using a phantom containing fat and aqueous protein solutions to simulate human spectra, but in the absence of glucose, these authors showed that if typical glucose tolerance test time profiles were used in assigning glucose concentrations to spectra within their phantom glucose data set that the PLS calibration models assessed with leave-one-out cross validation performed well; this is a very disturbing finding. In addition, they found that models developed with the leave-one-out cross-validation method were similar to those based on the use of an independent prediction set.

In order to establish validity of PLS models and their performance in specifically predicting glucose levels, some authors employ an examination of the regression coefficient vector.<sup>10</sup> We examined the vector and, using five latent variables, found generally narrow positive peaks at wavelengths characteristic of glucose absorption. For example, there was a positive peak around 1000 nm, weakly associated with glucose, and there was a further positive peak around 1620 nm, strongly associated with glucose. The presence of these positive peaks at these wavelengths indicates that they have positive correlations with glucose.

In our experimental protocol, we used glucose tolerance tests in order to change BGL levels. We then employed two methods for analyzing the collected 603 data sets. In method A, we randomly selected 402 data sets for calibration and used the remaining 201 data sets for prediction. In method B, we randomly selected 18 subjects, using all of their data for calibration and leaving the data from the remaining 9 subjects for prediction. The reasoning behind this was that random selection from the total data set, as in the method A, should reduce the possibility that the outcome of the analysis would be influenced by the time-correlated changes of BGL produced during the glucose tolerance test present in the data from an individual subject. By contrast, the outcome of the analysis based on the method B, where all of the data from each of the randomly selected 18 individual subjects were included, has the potential to be influenced by the time-correlated BGL changes. The results as analyzed using both the Bland-Altman method and the Clark error-grid were, however, very similar for methods A and B. This suggests that the time-correlated changes in BGL do not, in fact, have an influence on the analysis.

This first study has been to present the new method of pulse glucometry for the noninvasive BGL measurement along with the design of an accurate and high-speed spectrophotometer system and to evaluate the feasibility of this method using the limited spectral data sets with a multivariate calibration analysis. There is still much to be done to evaluate fully all aspects of this method.

The present instrumentation is laboratory-based and further development is required to investigate the feasibility of designing a small portable device suitable for patient use to achieve self-monitoring. It is also possible that the method could provide the possibility for noninvasive blood analysis of such substrates as triglyceride, albumin, cholesterol, glycated albumin, and so on. Further comprehensive studies will need to be carried out in order to investigate such possibilities.

## 6 Conclusions

We have described a new optical method, pulse glucometry, for noninvasive determination of BGL levels. A high-speed optical instrument has been successfully developed for gathering transmittance spectra from the adult human finger over the wavelength range of 900 to 1700 nm. We have been able to determine cardiac-related pulsatile changes in optical density and, using a PLS calibration model for glucose, we have subsequently been able to derive BGL estimates noninvasively in 27 healthy adult subjects during glucose tolerance tests. The results indicate that the technique can produce BGL estimates with acceptable precision and accuracy for clinical use. Since the present study is a first stage to validate the new method, further work is required to determine fully the performance of the instrument in diabetic subjects and also to assess the full potential of this method for clinical and research purposes.

## Acknowledgment

The authors would like to give their sincere thanks to Prof. Peter Rolfe, OBH Ltd., UK, for his valuable suggestions and comments on this work and for his assistance in preparing the manuscript. The authors would also like to thank Associate Professor Shinobu Tanaka, Masamichi Nogawa, and Dr. Takehiro Yamakoshi, for their technical assistance in this study. Financial support for this work was provided by SMC Corporation, Tokyo, Japan. SMC did not participate in the research in any way.

## References

1. J. N. Roe and B. R. Smaller, "Bloodless glucose measurements," *Crit. Rev. Ther. Drug Carrier Syst.* **15**, 199–241 (1988).
2. E. Csoregi, D. Schmidke, and A. Heller, "Design and optimization of a selective subcutaneously implantable glucose electrode based on wired glucose oxidase," *Anal. Chem.* **67**, 1240–1244 (1995).
3. D. Klonoff, "Non-invasive blood glucose monitoring," *Diabetes Care* **20**, 433–437 (1997).
4. J. Tamada, N. Bohannon, and R. Potts, "Measurement of glucose in diabetic subjects on non/minimally invasive transdermal extraction," *Nat. Med.* **1**, 1198–1201 (1995).
5. G. Rao, P. Glikfeld, and R. Guy, "Reverse iontophoresis: Noninvasive glucose monitoring *in vivo* in humans," *Pharm. Res.* **12**, 1869–1873 (1995).
6. J. Kost, S. Mitragotri, R. A. Gabbay, M. Pishko, and R. Langer, "Transdermal monitoring of glucose and other analytes using ultrasound," *Nat. Med.* **6**, 347–350 (2000).
7. D. C. Klonoff, "A review of continuous glucose monitoring technol-



- ogy," *Diabetes Technol. Ther.* **7**(5), 770–775 (2005).
8. M. R. Robinson, R. P. Eaton, D. M. Haaland, G. W. Koeppe, E. V. Thomas, B. R. Stallard, and P. L. Robinson, "Noninvasive glucose monitoring in diabetic patients: A preliminary evaluation," *Clin. Chem.* **38**(9), 1618–1622 (1992).
  9. H. M. Heise, "Applications of near-infrared spectroscopy in medical sciences," in *Near-Infrared Spectroscopy*, H. W. Siesler, Y. Ozaki, S. Kawata, and H. M. Heise, Eds., pp. 289 Wiley-VCH, Weinheim, Germany (2002).
  10. K. Maruo, M. Tsurugi, M. Tamura, and Y. Ozaki, "In vivo noninvasive measurement of blood glucose by near-infrared diffuse-reflectance spectroscopy," *Appl. Spectrosc.* **57**(10), 1236–1244 (2003).
  11. G. L. Cote, M. D. Fox, and R. B. Northrop, "Noninvasive optical polarimetric glucose sensing using a true phase measurement technique," *IEEE Trans. Biomed. Eng.* **39**, 752–756 (1992).
  12. B. Guclu, G. A. Engbretson, and S. J. Bolanowski, "Constrained optimization of Drude's equations eliminates effects of confounding molecules for the polarimetric measurement of glucose," *J. Biomed. Opt.* **9**, 967–977 (2004).
  13. R. Badugu, J. R. Lakowicz, and C. D. Geddes, "A glucose-sensing contact lens: From bench top to patient," *Curr. Opin. Biotechnol.* **16**(1), 100–107 (2005).
  14. O. S. Khalil, "Non-invasive glucose measurement technologies: An update from 1999 to the dawn of the new millennium," *Diabetes Technol. Ther.* **6**, 660–697 (2004).
  15. H. M. Heise, A. Bittner, and R. Marbach, "Clinical chemistry and near infrared spectroscopy: Technology for non-invasive glucose monitoring," *J. Near Infrared Spectrosc.* **6**, 349–359 (1998).
  16. A. M. Enejder, T. G. Secina, J. Oh, M. Hunter, W. Shih, S. Sasic, G. L. Horowitz, and M. S. Feld, "Raman spectroscopy for non-invasive glucose measurements," *J. Biomed. Opt.* **10**(3), 1–9 (2005).
  17. P. Rolfé, "In Vivo near infra-red spectrophotometry," *Annu. Rev. Biomed. Eng.* **2**, 315–354 (2000).
  18. M. A. Arnold and G. W. Small, "Noninvasive glucose sensing," *Anal. Chem.* **77**(17), 5429–5439 (2005).
  19. K. Yamakoshi, "A non-invasive blood constituent measuring instrument and measuring method," International Patent No. PCT/JP03/03587 (2003).
  20. A. B. Hertzman, "Photoelectric plethysmograph of the fingers and toes in man," *Proc. Soc. Exp. Biol. Med.* **37**, 529 (1937).
  21. T. Aoyagi, "Pulse oximetry: Its invention, theory, and future," *J. Anaesth.* **17**, 259–266 (2003).
  22. W. Nahm and H. Gehring, "Non-invasive in vivo measurement of blood spectrum by time-resolved near-infrared spectroscopy," *Sens. Actuators B* **29**, 174–179 (1995).
  23. H. M. Heise, A. Bittner, and R. Marbach, "Near-infrared reflectance spectroscopy for noninvasive monitoring of metabolites," *Clin. Chem. Lab. Med.* **38**(2), 137–145 (2000).
  24. T. Aoyagi, M. Kishi, K. Yamaguchi, and S. Watanabe, "Improvement of the ear piece oximeter," in 13th Meeting of the Japanese Society for Medical Electronics and Biological Engineering, pp. 90–91 (1974).
  25. T. Aoyagi, N. Kobayashi, and T. Sasaki, "Apparatus for determining the concentration of a light-absorbing material in blood," U.S. Patent No. 4,832,484 (1989).
  26. Y. Mendelson, R. A. Peura, and H. Harjunmaa, "Method and apparatus for monitoring blood analytes noninvasively by pulsatile photoplethysmography," U.S. Patent No. 5,137,023 (1992).
  27. K. H. Hazen, M. A. Arnold, and G. W. Small, "Measurement of glucose in water with first overtone near-infrared spectra," *Appl. Spectrosc.* **52**, 1597–1605 (1998).
  28. A. K. Amerov, J. Chen, G. W. Small, and M. A. Arnold, "Scattering and absorption effects in the determination of glucose in whole blood by near-infrared spectroscopy," *Anal. Chem.* **77**, 4587–4594 (2005).
  29. J. M. Bland and D. G. Altman, "Statistical methods for assessing agreement between two methods of clinical measurement," *Lancet* **1**, 307–310 (1986).
  30. W. L. Clarke, D. C. Cox, L. A. Conder-Frederick, W. Carter, and S. L. Pohl, "Evaluating clinical accuracy of systems for self-monitoring of blood glucose," *Diabetes Care* **10**, 622–628 (1987).
  31. H. M. Heise, "Glucose, in vivo assay of," in *Encyclopedia of Analytical Chemistry: Applications, Theory and Instrumentation*, R. A. Meyers, Ed., pp. 1–27, John Wiley & Sons, Ltd., New York (2000).
  32. P. Å. Öberg, "Optical sensors in medical care," in *Sensors in Medicine and Health Care*, P. Å. Öberg, T. Togawa, and F. A. Spelman, Eds., pp. 15–43, Wiley-VCH Verlag GmbH & Co. KGaA, Weinheim, Germany (2004).
  33. R. Haeckel, U. Brinck, D. Colic, H. U. Janka, I. Puntmann, J. Schneider, and C. Viebrock, "Comparability of blood glucose concentration measured in different sample systems for detecting glucose intolerance," *Clin. Chem.* **48**, 936–939 (2002).
  34. M. S. Patterson, B. Chance, and B. C. Wilson, "Time resolved reflectance and transmittance for the non-invasive measurement of optical properties," *Appl. Opt.* **28**, 2331–2336 (1989).
  35. J. R. Lakowicz and K. Berndt, "Frequency domain measurements of photon migration in tissues," *Chem. Phys. Lett.* **166**, 246 (1990).
  36. C. Abrahamsson, T. Svensson, S. Svanberg, S. Andersson-Engels, J. Johansson, and S. Folestad, "Time and wavelength resolved spectroscopy of turbid media using light continuum generated in a crystal fibre," *Opt. Express* **12**(17), 4103–4112 (2004).
  37. L. A. Sodickson, "Lateral tissue inhomogeneity: A missing link in photoplethysmographic noninvasive measurement of arterial blood constituents," *Clin. Chem.* **45**, 1687–1689 (1999).
  38. M. A. Arnold, J. J. Burmeister, and G. W. Small, "Phantom glucose calibration models from simulated noninvasive human near-infrared spectra," *Anal. Chem.* **70**(9), 1773–1781 (1998).